CONF-950856--1

SAND95-0518C

Hypervelocity Impact Phenomena

Lalit C. Chhabildas

Sandia National Laboratories, Experimental Impact Physics Department, P. O. Box 5800, Albuquerque, New Mexico 87185-0821, USA*

There is a need to determine the equations of state of materials in regimes of extreme high pressures, temperatures and strain rates that are not attainable on current two-stage light-gas guns. Understanding high-pressure material behavior is crucial to address the physical processes associated with a variety of hypervelocity impact events related to space sciences—orbital-debris impact, debris-shield designs, high-speed plasma propagation, and impact lethality applications. At very high impact velocities material properties will be dominated by phase-changes, such as melting or vaporization, which cannot be achieved at lower impact velocities. Development of well-controlled and repeatable hypervelocity launch capabilities is the first step necessary to improve our understanding of material behavior at extreme pressures and temperatures not currently available using conventional two-stage light-gas gun techniques. In this paper, techniques that have been used to extend both the launch capabilities of a two-stage light gas gun to 16 km/s, and their use to determine the material properties at pressures and temperature states higher than those ever obtained in the laboratory are summarized. The newly developed hypervelocity launcher (HVL) can launch intact (macroscopic dimensions) plates to 16 km/s. Time-resolved interferometric techniques have been used to determine shock-loading/release characteristics of materials impacted by such fliers as well as shock-induced vaporization phenomena in fully vaporized states. High-speed photography or radiography has been used to evaluate the debris propagation characteristics resulting from disc impact of thin bumper sheets at hypervelocities in excess of 10 km/s using the HVL. Examples of these experiments are provided in this paper.

1. INTRODUCTION

Until approximately four years ago, two-stage light-gas guns[1-3] produced the highest pressure and temperature states in material that can be achieved in the laboratory. This generally involves performing impact studies at impact velocities of 8 km/s using high impedance impactor materials such as tantalum or platinum. A suite of diagnostic and experimental techniques[4,5] are then used to measure material properties in the high-pressure, high-temperature shocked state induced in materials at these impact velocities. These techniques allow measurements of the shock-Hugoniot[6], shock-loading and release behavior[7-8], material strength[6-10], shock-induced melting,[8,11,12] and shock-induced vaporization[11-12] processes in materials. Exper-

* This work performed at Sandia National Laboratories, supported by the US Department of Energy under contract DE-AC04-94AL85000.

DISTRIBUTION OF THIS DOCUMENT IS UNLIMITED

MASTER

DISCLAIMER

Portions of this document may be illegible in electronic image products. Images are produced from the best available original document.

imental measurement of these material properties forms a data base needed to develop constitutive models to represent material behavior in dynamic loading[13].

For many space sciences applications, there is a requirement to extend the equations of state of materials to extremely high pressures, temperatures and strain rates to regimes not accessible by current two-stage light-gas guns. Many of these applications include orbital-debris impact[14,15], debris-shield designs[16-21], high-speed plasma propagation, and impact lethality effects[22-23]. At such high impact velocities material properties will be dominated by phase-changes, such as melting or vaporization, not routinely achieved at low impact velocities. Development of well-controlled and repeatable hypervelocity launch capabilities is the first step necessary to improve our understanding of material behavior in these regimes.

In this paper, techniques that have been used to extend the shocked material properties data base to pressures and temperature states higher than those previously obtained in the laboratory are described. In particular, the Sandia HyperVelocity Launcher[24-26] (HVL) which is capable of launching 0.5 mm to 1.0 mm thick by 6 mm to 19 mm diameter plates to velocities approaching 16 km/s, will be briefly described. Recent results of interferometric particle-velocity measurements of shock loading and release in aluminum and titanium at impact velocities of 10 km/s which use the HVL will be reported. Techniques developed to probe the kinetics of shock-induced vaporization of a thin zinc plate[27] shocked to 5.5 Mbar resulting from an initial tantalum impact at over 10 km/s will also be discussed. An example of a debris cloud resulting from impact of an aluminum flier plate on a thin aluminum bumper shield[28] at velocities of 10 km/s will also be described. Most significantly, these experiments demonstrate the feasibility of using the hypervelocity launcher to determine material properties in pressure and temperature regimes that have never been accessible by experimental methods. Experimental measurement of these material properties will lead to the development and validation of constitutive models for material behavior that are needed for hydrodynamic code calculations[29-30] for many programmatic needs for space sciences and lethality assessments.

2. HYPERVELOCITY LAUNCHER (HVL)

The principle of operation of the Sandia HyperVelocity Launcher (HVL) is briefly described here. Very high driving pressures (tens or hundreds of GPa), are required to accelerate flier plates to hypervelocities. This loading pressure pulse on the flier plates must be time-dependent to prevent the plate from melting or vaporizing. This is accomplished by using graded-density impactors[9,10,31]. When this graded-density material is used to impact a flier-plate in a modified two-stage light gas gun, as indicated in Figure 1(a), nearly shockless, megabar pressures are introduced into the flier plate[10,26]. The pressure pulse must also be tailored to prevent spallation of the flier-plate. This technique has been used to launch nominally 1-mm-thick aluminum, magnesium and titanium (gram-size) intact plates to 10.4 km/s[24] and 0.5-mm-thick aluminum and titanium (half-gram size) intact plates to 12.2 km/s[25]. More recently the technique has been enhanced by using the experimental configuration described in Figure 1(b) to allow the launching of titanium and aluminum plates to velocities approaching 16 km/s[26]. The experimental design shown in Figure 1(b) acts as a dynamic acceleration reservoir which further enhances the flier plate velocity[26]. This is the highest mass-velocity capability attained with laboratory launchers to date, and therefore should open up investigations into new regimes of impact physics using a variety of diagnostic tools[4,5,32].

DISTRIBUTION OF THIS DOCUMENT IS UNLIMITED

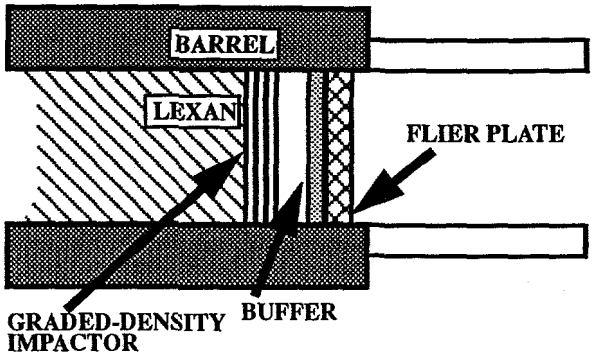

Figure 1(a). The Hypervelocity Launcher (HVL). Configuration used to launch flier plates to hypervelocities.

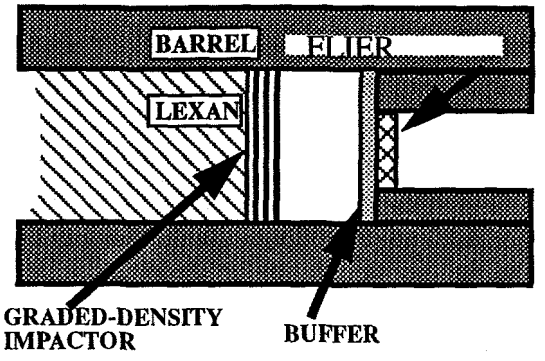

Figure 1(b). Enhanced HyperVelocity Launcher, (EHVL). Configuration used to launch confined flier plates in a tungsten barrel to hypervelocities.

Due to the severe loading conditions which result from time-dependent megabar loading pressures, the flier plate achieves peak velocities over tens of millimeter acceleration distances. The plate appears to be "flat" for approximately the first thirty millimeter flight distances (see Figure 2(a)), and will then generally "bow" with increasing flight path. Flier plates have been launched intact and radiographed to flight distances of 1.4 meters from launch[26] with this technique as indicated in Figure 2(b). Even though shockless loading conditions are used to accelerate the flier plate, the final temperature of the flier plate upon acceleration is approximately 600 K for the geometry used in Figure 1(a) after achieving velocities of 10 km/s. This is "cold" compared to its melt temperature, despite using enormous energy (compared to its melt and vaporization energy) to achieve hypervelocities. Designs using lower-impedance buffers such as foam can further reduce the temperature of the accelerating flier-plate.

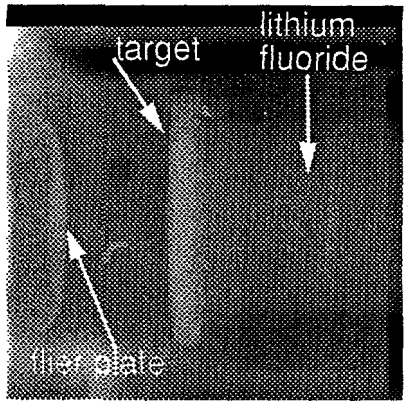

Figure 2(a). Radiograph of a titanium flier-plate (prior to impacting a titanium target). The flier-plate is traversing at 9.60 km/s

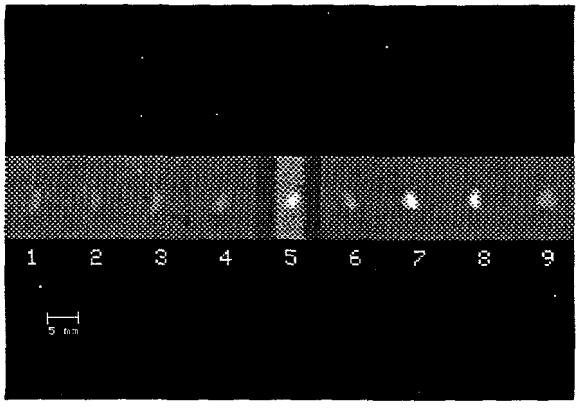

Figure 2(b). Radiographs of a titanium flier-plate traversing from left to right at a speed of 14.4 km/s over a flight distance of 1400 mm.

3. APPLICATIONS

We have used the hypervelocity launcher (HVL) to perform one-dimensional plate-impact experiments. To achieve one-dimensional conditions, the target plate is stationed ~ 20 mm from the flier-plate. This ensures that the flier plate achieves peak particle velocity prior to impact, and remains relatively flat (see Figs. 2(a) & 5(a)) prior to impact. No attempt has been made to date to characterize the *planarity* of the impacting flier plate. The experimental configuration used to perform shock-loading and release measurements and shock-induced vaporization experiments are shown in Figure 3(a) and 3(b), respectively.

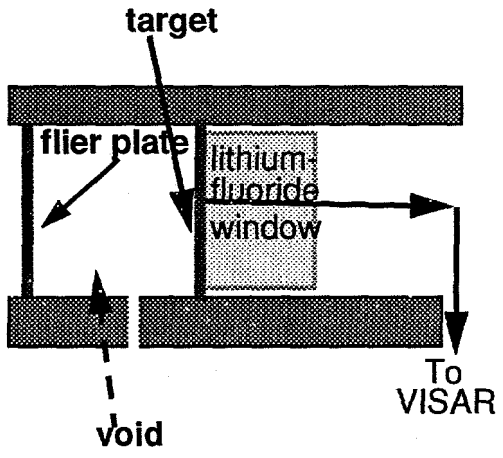

Figure 3(a). HVL configuration for shock-loading and release experiments. Resultant loading and release is measured as particle-velocity history at the target lithium-fluoride window interface.

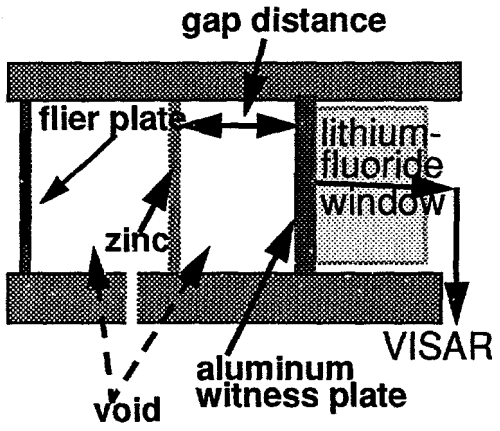

Figure 3(b). HVL configuration for vaporization experiments. The stagnation velocity history resulting from vaporized zinc is measured at the target lithium-fluoride window interface.

3.1 Shock-Loading and Release Experiments

The experimental configuration used to determine the shock loading and release states is described in Figure 3(a). Symmetric plate-impact experiments have been performed using aluminum, titanium, and tantalum at impact velocities of ~ 10 km/s. Figure 2(a) shows the radiograph of an experiment in which a 0.56 mm titanium alloy (Ti-6Al-4V) flier-plate is launched at 9.6 km/s prior to impacting a 2.0 mm thick titanium alloy target. The lithium-fluoride window[32] is clearly seen in the radiograph in Figure 2(a). The flat portion of the flier-plate prior to impact as observed in the radiograph is 19 mm. Note that for the full duration of the experiments there is a void behind the flier-plate; this allows measurements of a complete release from the shocked state. As indicated in Figure 3(a), a velocity interferometer VISAR[33], is used to estimate the particle-velocity history at the sample/lithium-fluoride window interface. The time-resolved particle velocity history measurements at the target/lithium-fluoride window interface are shown in Figure 4(a) and 4(b) for aluminum and titanium, respectively. Since no fiducial was established in these experiments, the shock arrival time at the target/window-interface is arbitrarily set to zero.

Figure 4(a) depicts the shock loading and release profile in aluminum shocked to over 1.6 Mbar at an impact velocity of 9.95 km/s. In this experiment, a 0.98 mm thick aluminum flier-plate impacts a 1.98 mm thick aluminum target. Notice that a sustained shock of approximately 80 ns is observed in the figure prior to release. The titanium alloy is shocked to 2.3 Mbar at an impact velocity of 9.6 km/s, and a complete release profile as indicated in Figure 4(b) is measured. A profile resembling wave attenuation is measured in the titanium experiment because a thin flier plate (0.56 mm) impacts a thick (2.0 mm) target. Both experiments indicate a lack of elastic-plastic release structures—a clear indication of complete melt. Most significantly, the results demonstrate the successful use of time-resolved velocity interferometric techniques for EOS investigations using the HVL. These release profile structures then determine the off-Hugoniot states of materials shocked to extremely high-pressures.

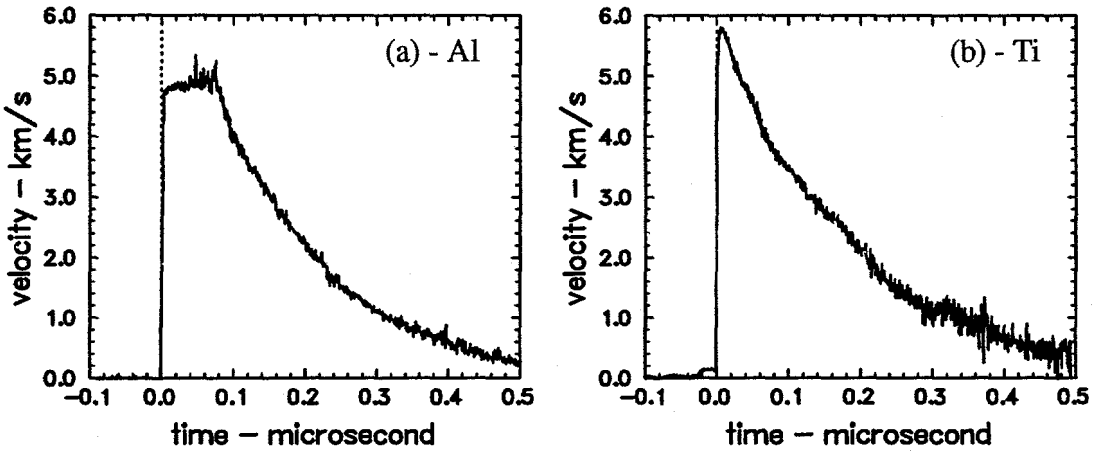

Figure 4. Measured interface particle velocity history for shock-loading and release experiments in (a) 6061-T6 aluminum at an impact velocity of 9.95 km/s, and (b) Ti-6Al-4V alloy at an impact velocity of 9.6 km/s. Symmetric impact configuration was used in both experiments.

Lithium-Fluoride Window Transparency: The successful measurements reported in Figure 4, demonstrate the transparency of the lithium-fluoride window at much higher pressures (and temperatures) than this window material has ever been subjected to before[32], *i.e.*, to 1.6 Mbar and 2 Mbar, respectively, in the aluminum and titanium experiment. Previous study has demonstrated transparency of lithium fluoride (LiF) windows to stresses of 1.2 Mbar[32]. A symmetric impact experiment at 10 km/s using both tantalum as a target and as a flier plate, however, did not yield a release profile measurement similar to those in Figure 4. This corresponds to a stress of ~ 8 Mbar in tantalum and 3 Mbar in the LiF window. This pressure level causes an apparent transparency loss in the LiF window. More experiments are needed, however, to further resolve this issue. This work also points to the need to develop new time-resolved techniques to allow successful measurements of off-Hugoniot states at extremely high pressures.

3.2 Shock-Induced Vaporization Experiments

This section briefly describes the use of the hypervelocity launcher to probe the kinetics of the shock-induced vaporization process in materials[27]. These results represent the first time-resolved measurements of full vaporization in zinc[27] resulting from release from stress states

over the range of 3 Mbar to 5.5 Mbar, and temperatures as high as 39,000 K (3.4eV) in the zinc target[27]. (The release isentrope computed from a shock pressure of 5.5 Mbar and 39,000 K pass near the zinc critical point and it is therefore believed that full vaporization of zinc target occurs.) The experimental schematic is indicated in Figure 3(b), while the radiographs of the experiment are depicted in Figure 5(a). Following the arrival of the compressive wave at the free surface of the zinc target, a decompression wave propagates back into the zinc sample, which is now in a mixed phase of liquid and vapor. The rarefied liquid-vapor products left in the wake of this wave traverse a gap of known dimensions and stagnate against an aluminum witness plate backed by a lithium-fluoride laser-interferometer window[32]. The stagnation velocity history is determined through the use of a velocity interferometer [33], VISAR. Measured time-resolved stagnation particle velocity histories of experiments conducted at an impact velocity of 10.1 km/s are shown in Figure 5(b). In these experiments[27] the vaporized products are allowed to traverse gap distances of up to 20 mm.

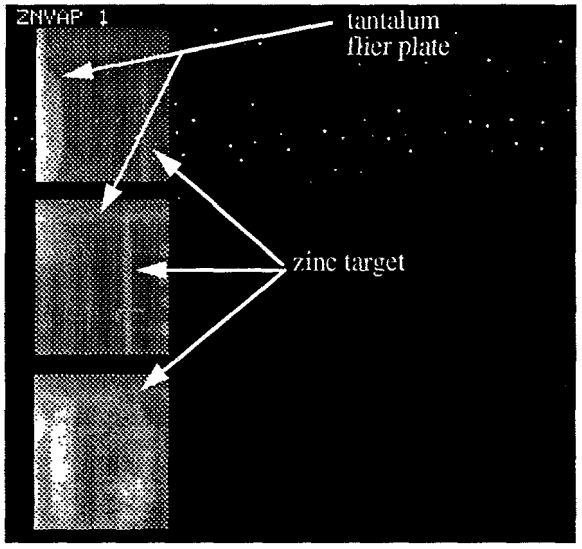

Figure 5(a). Radiographs of a tantalum flier-plate launched to velocities of 10.1 km/s prior to impacting a zinc target in the final frame using HVL.

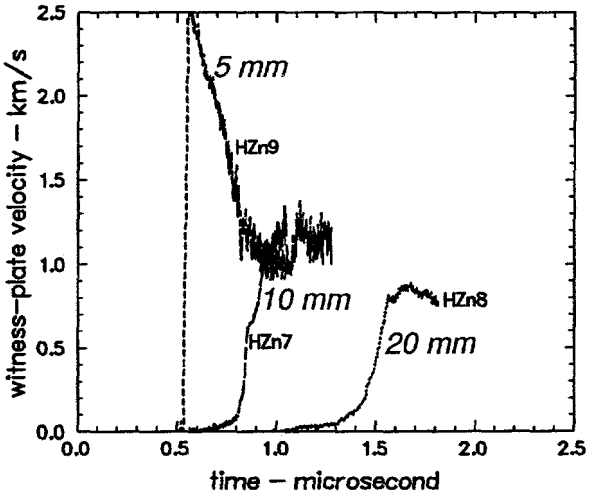

Figure 5(b). Measured stagnation particle velocity histories of shock-induced vaporization experiments conducted at an impact velocity of 10.1 km/s.

Stagnation particle velocity measurements: In both sets of experiments conducted at 9.1 km/s and 10.1 km/s, the measured peak particle velocity produced by the liquid-vapor states stagnating at the aluminum witness plate depends on the propagation distance (*i.e.*, on gap size). The change in peak witness-plate velocity u_{wp} with respect to gap size is a strong indication of the amount of vaporization that occurs in the zinc over the time duration of the experiment. Figure 6 shows the variation of u_{wp}, with respect to gap size. u_{wp} is normalized with respect to the tantalum impact velocity V, and zero-gap velocity U_{max}, respectively, where U_{max} is the peak witness-plate velocity for a gap size of zero. The value of U_{max} is based on calculations.

The aluminum witness-plate/lithium-fluoride window can be regarded as a target with which the liquid/vapor debris cloud interacts. The peak interface velocity measurement u_{wp} is

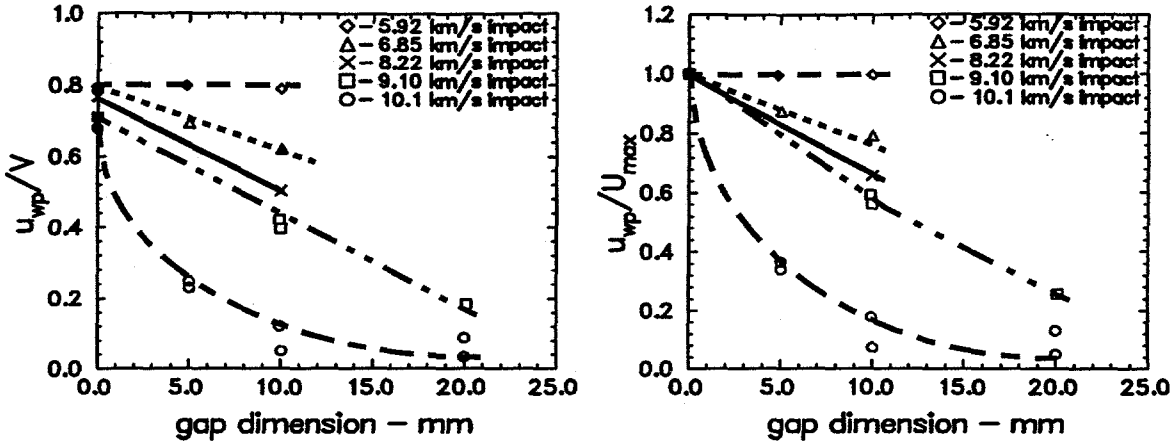

Figure 6. Normalized measured witness-plate peak velocity vs. propagation distance (i.e., gap size). The normalized factors are (a) tantalum impact velocity V and (b) the computed zero-gap peak velocity Umax (which depends on tantalum impact speed and experiment geometry.

an indicator of the maximum stress resulting from this interaction. Observe that u_{wp}/V or u_{wp}/U_{max}, are *higher* for the *lower*-speed 9.1 km/s shots than for the corresponding 10.1 km/s shots, which suggests that greater vaporization occurred in the 10.1 km/s shots. Figure 6, which summarizes all experimental data[27,36] shows that the peak witness-plate velocity u_{wp} and, therefore, the target/debris interaction stress, decrease monotonically with increasing propagation distance (gap size). All curves in Figure 6 must — in one-dimensional theory — asymptote to some constant value as gap size is increased. When such a curve asymptotes to *zero*, the sample must have vaporized completely. When a curve asymptotes to some non-zero value of u_{wp}/U_{max}, the sample must have only partially vaporized. When a curve is *constant*, no vaporization must have occurred and the maximum interaction stress must be independent of gap size. In Figure 6, the lowest speed experiment[36] (5.92 km/s) exhibits negligible expansion (*i.e.*, the zinc target remains essentially intact as it crosses the gap). By contrast, the highest speed (10.1 km/s) experiment[27] shows considerable expansion of the zinc, which corresponds to a much lower stress on the buffer than the lower-speed lower-vaporization experiments. (Even though loading stress can be reduced substantially by vaporization, the survivability of any target nevertheless depends on many other parameters including the duration of the pressure pulse, the thickness of the target, and the yield and fracture strength of the target.) For zinc, the rapid approach to an asymptotic limit suggests that boiling occurs more rapidly from super-critical states.

Although not specifically discussed in this paper, the experiments have suggested a lack of agreement with CTH code calculations[34] using an existing ANEOS equation of state[35]. It should also be noted that the same ANEOS model, however, describes the impact experiments on zinc performed at lower impact velocities of 5.8 km/s to 7 km/s[36] quite satisfactorily. This clearly indicates a need to develop and/or refine current EOS models for zinc which describe the shock-induced vaporization process in extreme pressure and temperature regimes.

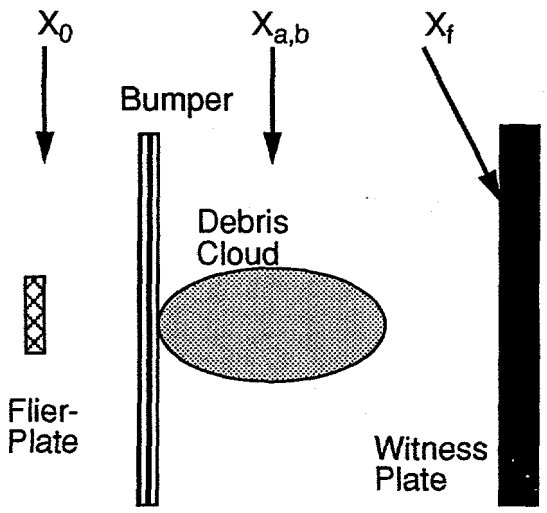

Figure 7. Experimental schematic indicating the set up used for debris propagation studies.

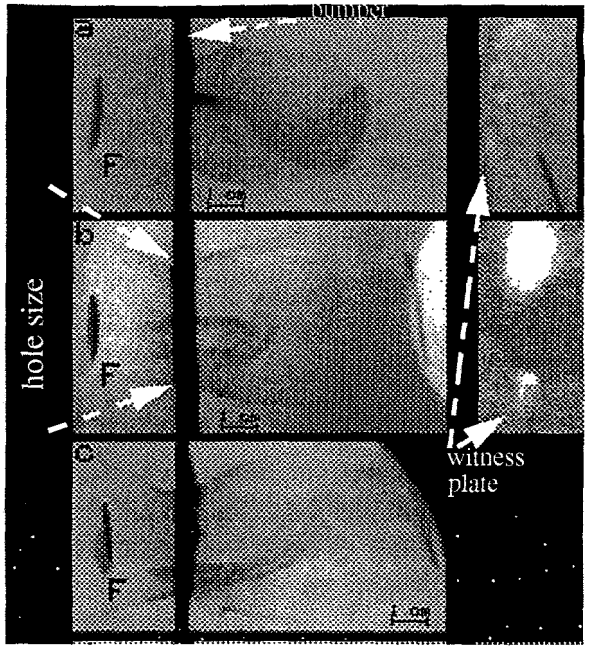

Figure 8. Radiographs of the debris cloud formed upon impact of an aluminum flier plate F with an aluminum bumper at (a) 5 km/s, (b) 7.43 km/s and (c) 9.56 km/s.

3.3 Debris Cloud Studies

In this section, an experimental technique used to perform two-dimensional experiments on the HyperVelocity Launcher (HVL)[24-26] is described. The experimental configuration is indicated in Figure 7. Aluminum flier plates 17-mm diameter by 0.92-mm thick were accelerated to velocities over the range of 5 to 11 km/s and, as indicated in Figure 8, were radiographed prior to impact on 1.27 mm thick aluminum bumper plates. Aluminum witness plates 3.18 mm thick were positioned 203 mm behind the bumper plate. The debris cloud generated upon impact is viewed between the bumper shield and the witness plate using flash X-ray techniques. The back surface of the witness plate was also radiographed at an angle to determine the effect of subsequent loading (on the witness plate) by the impact-generated debris cloud. The X-ray measurements of the flier-plate prior to impact, debris cloud, and the subsequent witness plate rupture are all indicated in Figure 8. Only those X-rays that are not absorbed by the debris cloud, *i.e.*, the relatively higher density material within the cloud, are imaged.

Assuming a flat-plate impact, the peak stress states in the aluminum flier and the bumper are ~ 58 GPa, 102 GPa, 150 GPa, and 190 GPa at impact velocities of 4.99, 7.43, 9.56, and 11.1 km/s, respectively. The corresponding release temperatures of aluminum[37] shocked to 60 GPa are very close to the melt temperature of 930 K, while the release temperature of aluminum that has been shocked to 190 GPa is over 3000 K. This is well above its boiling temperature of 2700 K. Therefore, the aluminum debris will be in the solid/liquid phase at an impact velocity of 5 km/s, liquid phase at 7.43 km/s, and liquid phase with increasing vapor fraction at the higher impact velocities of 9.56 and 11.1 km/s, respectively.

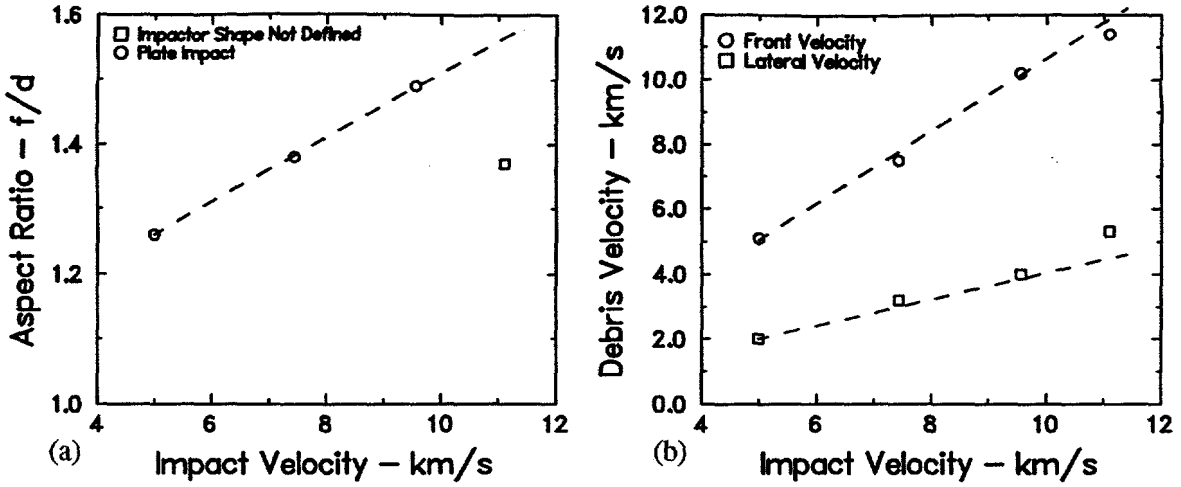

Figure 9. (a) The variation of the aspect ratio (ratio of the leading edge of the debris front f to its diameter d) with impact velocity and (b) the variation of the debris front velocity and lateral velocity with impact velocity.

Debris Cloud Shape: The flier-plate mass used in this study is ~ 0.53 g, and its undeformed *aspect ratio, i.e.*, thickness-to-diameter ratio is ~ 0.05. After impact, the free-surface stress relief dominates. The diameter of a sphere representing an equivalent mass of the flier-plate is 7.2 mm. The wave interaction time for a plate impact will be one-eighth the time compared to a spherical impact. Therefore, one-dimensional effects control the initial impact interaction. This is indicated by the shape of the debris cloud observed in the radiographs. The leading edge of the debris cloud in all instances has the highest density mass. The shape of the debris cloud generated upon impact is found to depend on the flier-plate tilt. The data indicate a central core of higher density surrounded by a diffused layer. The variation of the aspect ratio with impact velocity is shown in Figure 9. If the debris propagation effects are influenced strictly by one-dimensional processes, then this ratio is expected to increase with time. For spherical propagation, this ratio is expected to be close to unity[38].

Solid fragments are observed in Figure 8 for the impact experiment at 5 km/s. It is surprising to observe a disc shaped leading edge for the two experiments at 7.44 km/s and 9.56 km/s, considering that the bumper material is expected to be completely molten. Any low density vapor preceding the debris cloud is not observable on the radiographs. It can be shown that low density debris of approximately 0.008 g/cm^3 would uniformly fill into a cylinder having an aspect ratio of 1.42. This defines the need for low energy X-ray sources to accurately/precisely define the true "shape" of the debris cloud.

Debris Cloud Propagation Velocities: The debris front and lateral velocities of the experiments are indicated in Figure 9. As indicated in the figure, the high density leading edge of the debris front is travelling faster than the impact velocity. Previous impact experiments performed at 10 km/s (diagnosed using fast framing photographic techniques[17-18]) have indicated a vapor front (preceding the debris cloud) travelling at velocities of 14 km/s. It is, therefore, crucial that both X-rays and photography be used, if possible, to obtain a detailed description of the debris cloud. The lateral velocity of the debris cloud resulting from plate impact also increases with impact velocity; when expressed as a fraction of the impact velocity, the lateral velocity appears to be relatively constant and ~ 40% of the impact velocity. Note the radial expansion velocity will be ~ 20% of the impact velocity.

The hole size in the bumper plate is estimated from the radiographs to be ~ 26.5 mm and is independent of the impact velocity when the integrity of the flier-plate is maintained. When compared to the original flier-plate dimensions of 17 mm, this is an amplification by a factor of 1.5 to 1.6 in these studies. It should be noted that although there is both molten and vaporized aluminum in the debris cloud, the backwall is still ruptured—mainly because of the high-density leading edge and the presence of what appears to be a central/collimated high density core.

4. SUMMARY

Examples of one- and two-dimensional experiments described in this report demonstrate the feasibility of using the hypervelocity launcher to determine material properties in pressure and temperature regimes that have never been accessible in the laboratory before. Only a brief summary is presented here to illustrate the use of HVL and time-resolved techniques for material properties measurements. The reader is encouraged to refer to the original articles for experimental details and experimental impact conditions. These experiments, due to their plate geometry, will also serve to validate hydrodynamic codes in the impact regime (where very few experiments are available) not only for well-controlled EOS studies but also for ballistic applications.

It should be emphasized that most of the techniques used are those that were developed earlier for relatively lower impact studies. There is, however, a need for the development of techniques that would have better spatial resolution or time resolution that is commensurate with the physical processes that are being diagnosed. It is anticipated that successful experimental measurement of the material properties and the physical processes related to hypervelocity impact will eventually lead to the development and validation of constitutive and EOS models for material behavior that are needed for hydrodynamic code calculations for many programmatic needs including lethality assessments.

Acknowledgments

The author would like to acknowledge W. D. Reinhart, C. A. Hall for their able technical support in conducting these experiments, R. M. Brannon for calculational analysis/simulation of the shock-induced vaporization experimets in zinc, and E. S. Hertel, Jr., and T. G. Trucano for their careful review and constructive comments of this paper.

REFERENCES

1. J. R. Asay, L. C. Chhabildas and L. M. Barker, Sandia National Laboratories Report SAND85-2009, (1985) (unpublished).
2. A. C. Charters, Int., J. Impact Engng., V5 (1987) 181.
3. L. C. Chhabildas, in Recent Trend in High-Pressure Research, Proceedings of the XIII AIRAPT Conference on High Pressure Science and Technology, ed. by A. K. Singh, Bangalore, India, (1992) 739.
4. L. C. Chhabildas, Int., J. Impact Engng., V5 (1987) 205.
5. L. C. Chhabildas, and R. A. Graham, in AMD Vol. 83, ed., by R. Stout, F. Norwood, and M. Fourney, (1987) 1.

6. See for example LASL Shock Hugoniot Data, ed., by S. P. Marsh, University of California, Press, (1980).
7. J. R. Asay and L. C. Chhabildas, in Shock Waves and High-Strain-Rate Phenomena in Metals, Plenum Publishers, New York (1981).
8. J. R. Asay, L. C. Chhabildas, G. I. Kerley and T. G. Trucano, in *Shock Waves in Condensed Matter-1985*, ed. by Y. M. Gupta, Plenum Publishers, (1986) 145.
9. L. C. Chhabildas, L. M. Barker, J. R. Asay and T. G. Trucano, Int. J. Impact Engng., V10 (1990) 107.
10. L. C. Chhabildas and J. R. Asay in Shock Waves and High-Strain-Rate Phenomena in Materials, Marcel Decker, New York (1992) 947.
11. J. R. Asay, T. G. Trucano and L. C. Chhabildas, in *Shock Waves in Condensed Matter-1987*, ed. by S. C. Schmidt, J. W. Forbes and N. C. Holmes, Elsevier Science Publishers, (1988) 159.
12. J. R. Asay, T. G. Trucano and R. S. Hawke, Int. J. Impact Engng., V10, (1990) 51.
13. J. R. Asay and G. I. Kerley, J. Impact Engng., V5, (1987) 69.
14. Report on Orbital Debris by Interagency Group (Space) for National Security Council, Washington, D.C., (1989).
15. D. J. Kessler, R. C. Reynolds and P. D. Anz-Meador, NASA TM 100-471, (1989).
16. F. L. Whipple, Astronomical J., No. 1161, (1947) 131.
17. L. C. Chhabildas, E. S. Hertel, S. A. Hill, in *Shock Waves in Condensed Matter-1991*, ed. by S. C. Schmidt, R. D. Dick J. W. Forbes and D. G. Tasker, Elsevier Science Publishers, (1992) 991.
18. L. C. Chhabildas, E. S. Hertel, S. A. Hill, in *Proceedings of the Hypervelocity Impact Symposium-1991*, University of Kent at Canterbury, Kent, U.K., ed. by J. A. M. McDonnel (1992) 247.
19. J. A. Ang, L. C. Chhabildas, B. G. Cour-Palais, E. C. Christiansen and J. L. Crews, Space Programs and Technologies Conference, AIAA Paper 92-1590 (1992).
20. B. G. Cour-Palais, Int. J. Impact Engng., Vol. 10, (1990) 221.
21. M. B. Boslough, J. A. Ang, L. C. Chhabildas, B. G. Cour-Palais, E. C. Christiansen, J. L. Crews, W. D. Reinhart, and C. A. Hall, Int. J. Impact Engng., V14, (1993) 95.
22. L. N. Kmetyk, L. C. Chhabildas, M. B. Boslough and R. J. Lawrence, Sandia National Laboratories Report, SAND94-0878, 1994.
23. R. J. Lawrence, L. N. Kmetyk and L. C. Chhabildas, Int., J. Impact Engng., V17, (1995).
24. L. C. Chhabildas, L. M. Barker, J. R. Asay, T. G. Trucano, G. I. Kerley and J. E. Dunn, in *Shock Waves in Condensed Matter-1991*, ed. by S. C. Schmidt, R. D. Dick, J. W. Forbes and D. G. Tasker, Elsevier Science Publishers, (1992) 1025.
25. L. C. Chhabildas, J. E. Dunn, W. D. Reinhart and J. M. Miller, Int. J. Impact Engng., V14, (1993) 121.
26. L. C. Chhabildas, L. N. Kmetyk, W. D. Reinhart and C. A. Hall, Int. J. Impact Engng., V17, (1995).
27. R. M. Brannon and L. C. Chhabildas, Int., J. Impact Engng., V17, (1995).
28. L. C. Chhabildas, M. B. Boslough, W. D. Reinhart and C. A. Hall, in *AIP Conference Proceedings 309*, V2, (1994) 1841.

29. L. C. Chhabildas, W. D. Reinhart and C. A. Hall, Space Programs and Technologies Conference, AIAA Paper 94-4538 (1994).
30. L. C. Chhabildas and T. G. Trucano, ICES Proceedings (1995).
31. L. M. Barker, in *Shock Waves in Condensed Matter-1983*, ed. by J. R. Asay, R. A. Graham, and G. K. Straub, Elsevier Science Publishers, (1984) 217.
32. J. L. Wise and L. C. Chhabildas, in *Shock Waves in Condensed Matter-1985*, ed. by Y. M. Gupta, Plenum Publishers, (1986) 441.
33. L. M. Barker and R. E. Hollenbach, J. Appl. Phys., 43 (1972) 4669.
34. J. M. McGlaun, F. J. Zeigler, S. L. Thompson and M. G. Elrick, Sandia National Laboratories Report SAND88-0523, (1988).
35. S. L. Thompson, Sandia National Laboratories Report SAND89-2951, May (1990).
36. J. L. Wise, G. I. Kerley, T. G. Trucano, ed. by S. C. Schmidt, R. D. Dick, J. W. Forbes and D. G. Tasker, Elsevier Science Publishers, (1992) 61.
37. G. I. Kerley, Int., J. Impact Engng., V5, (1987) 441.
38. C. H. Konrad, L. C. Chhabildas, M. B. Boslough, A. J. Piekutowski, K. L. Poormon, S. A. Mullin and D. L. Littlefield, High-Pressure Science and Technology-1993, AIP Conference Proceedings 309, V2, (1994) 1845.